Two-dimensional electronic structure of the adsorbate system N/Cu(100): Photoelectron spectroscopy and one-step model calculations

T. Michalke,[1] R. Matzdorf,[1] J. Braun,[2] and A. Postnikov[3]
[1]*Institut für Physik, Universität Kassel, 34132 Kassel, Germany*
[2]*Institut für Mathematik und Angewandte Informatik, Universität Hildesheim, 31141 Hildesheim, Germany*
[3]*Paul Verlaine Universität-LPMD/IPC, 57078 Metz, France*

(Received 17 May 2006; revised manuscript received 18 March 2008; published 23 April 2008)

In this paper, we present a detailed study of the electronic structure of the adsorbate system Cu(100)$c(2\times2)$N by using angle-resolved ultraviolet photoelectron spectroscopy. The measured spectra reveal a variety of complex multipeak structures below the Fermi level. The adsorbate-derived states, which are of special interest, have been selected from the Cu-induced peaks by varying the polarization angle of the linear polarized light. The experimental analysis is supported by self-consistent electronic structure calculations within the density functional theory in order to determine the symmetry properties of the different adsorbate states. Due to the direct comparison with calculated photoemission spectra, a quantitative analysis of the surface geometry was possible. A structure model with outward relaxation of the first layer and twofold symmetry caused by combined rumpling of Cu and N atoms within this layer is favored by our investigation.

DOI: 10.1103/PhysRevB.77.165425 PACS number(s): 73.20.−r, 75.70.Rf, 75.50.Bb, 79.60.−i

I. INTRODUCTION

The adsorbate system Cu(100)$c(2\times2)$N has triggered a variety of experimental and theoretical investigations[1] because at this surface, self-organized nanostructures with a typical size of 5×5 nm^2 have been observed. They induce a novel morphology of the surface,[2] which may serve, for example, as a template for self-organized growth of magnetic nanostructures.[3] In this context, a quantitative controlling of the growth process is essential. Moreover, material design of nanostructures is intimately connected with a quantitative understanding of the structural properties as well as of the corresponding electronic structure. However, the geometric structure of Cu(100)$c(2\times2)$N is still not completely clarified. Two structure models have been introduced, but neither of them can quantitatively explain all low-energy electron diffraction (LEED)-IV data. The reason for this deficit in experimental information may be found in a strong lattice deformation at the boundaries of the N islands. Also, the electronic band structure has not been studied in detail so far. Only the local density of states of the adsorbate system was investigated,[4] and a single band structure calculation is found in the literature.[5]

This study presents a series of angle-resolved photoemission measurements of the adsorbate system Cu(100)$c(2\times2)$N in combination with a detailed analysis of the two-dimensional electronic band structure. In our experiments, we used linear polarized ultraviolet light, which allows for a quantitative symmetry analysis of the different adsorbate-induced states. To achieve a reliable interpretation of the experimental spectra, we additionally performed electronic structure as well as photocurrent calculations in the framework of the relativistic one-step model of photoemission. The paper is organized as follows. Section II is devoted to the experimental details. An introduction to the electronic structure and one-step photoemission calculations follows in Sec. III. In Sec. IV, we discuss the experimental valence band spectra and compare with two-dimensional band structure results and theoretical photoemission data. A summary is given in Sec. VI.

II. EXPERIMENTAL DETAILS

A. Preparation

The experiments were performed in an ultrahigh vacuum system with typical base pressures of less than 2×10^{-10} mbar. The ultraviolet light source is equipped with a rotatable polarizer arrangement that allows a continuous variation of the polarization angle between $\alpha=0°$ (p polarized) and $\alpha=90°$ (s polarized) with respect to the incidence plane. The incidence angle ψ is fixed to 45° with respect to the analyzer direction ($\psi=45°$ at $\theta=0°$). This arrangement results in a variation of the incidence angle when changing the electron emission angle θ, whereas the light incidence and electron emission directions are confined to the same optical plane. The electron energy analyzer provides an energy resolution down to $\Delta E\approx20$ meV and is equipped with a self-built lens system, which guarantees a variation in the angular resolution between $\Delta\theta=\pm0.2°$ and $\pm1.5°$.

The sample (oriented to $\pm0.3^{\circ}$) was mechanically polished and cleaned *in situ* by repeated cycles of Ar-ion bombardment and subsequent annealing. Since N_2 does not chemisorb on Cu at room temperature, we have prepared the adsorbate layer by N_2-ion bombardment (2×10^{-5} mbar N_2 99.999% purity at a beam energy of 200 eV for different time intervals) and subsequent annealing at 680 K.

During the deposition procedure, the sample current was measured in order to control the surface coverage. Furthermore, the coverage was controlled by photoemission measurements of the work function ϕ, which depends on the amount of the deposited N. The work function was calculated from the onset of the secondary electrons with respect to the Fermi energy measured with a negative bias voltage at the sample. The work function was found to be 4.70 ± 0.04 eV for the clean Cu(100) surface and 5.07 eV for

the full coverage of half a monolayer. The islands, which coalesce at this coverage, show strain-induced trenches along the [011] directions.[6] In order to achieve the squared island formation, a smaller coverage with $\phi \approx 4.97 \pm 0.05$ eV was chosen.

B. Low-energy electron diffraction

On a flat Cu(100) surface, the N atoms form square islands of about 5×5 nm^2 in size. The driving force for this self-organized patterning is found in the relaxation process of the elastic strain. In detail, the induced elastic strain is relieved by expanding the adjacent Cu lattice as a reaction of the incommensurate $c(2 \times 2)$N overlayer structure.[7] Ohno *et al.* were able to show by scanning tunneling microscopy (STM) measurements that the Cu lattice is inhomogeneously distorted. They found a compressed lattice at the clean Cu areas, an increased lattice constant at the island boundaries, and almost a bulk periodicity at the island centers.[8]

The structural properties of atomic N on Cu(100) have been studied by various methods including LEED,[9,10] surface-extended x-ray-absorption fine structure,[11] electron-energy-loss spectroscopy,[12] photoelectron diffraction,[13] and STM.[1] All measurements agree in the fact that the N atoms are located in the fourfold hollow sites. Also, a possible reconstruction of the Cu atoms within the first atomic layers[14] could be determined from the experimental data. A rumpled surface has been proposed, in which the adsorbate sites show a twofold symmetry behavior only.[13,15] The reconstruction involves a strong periodic distortion of the outermost Cu layer perpendicular to the surface with the additional appearance of different domains with opposite parity.

The quality of the sample preparation has been checked by LEED. At all different coverages, a sharp LEED pattern of the $c(2 \times 2)$ structure was observed. For low coverages between 0.25 and 0.4 ML, additional spots appeared belonging to the characteristic island structure shown in Fig. 1. The reciprocal distance of these spots corresponds to an average island distance of 5.8 ± 0.5 nm. At saturation coverage (0.5 ML), the islands coalesce and trenches accompanied by lines appear on the surface in the [011] directions. These lines show up because the coherence length of the electrons is smaller than the length of the trenches.

C. Angle-resolved ultraviolet photoemission spectroscopy

The electronic structure of the adsorbate system was measured for a surface covered by square islands, showing a work function of less than 5.07 eV. The measurements were performed for different polarization directions of the UV light and for different photon energies. The discharge lamp was either used with He, Ne, or Ar, He: $\hbar\omega = 21.22$ eV, Ne: 16.85 eV/16.67 eV, and Ar: 11.83 eV/11.62 eV. In most cases, a superposition of two peaks excited by the two different photon energies (for Ne or Ar) has been observed, but only for a very small linewidth, these two peaks can be distinguished.

The Tamm surface state observable on the clean Cu(100) at $\bar{M}$ vanishes after deposition for coverages with a work function $\phi \geq 4.95$ eV. On the other hand, adsorbate-induced

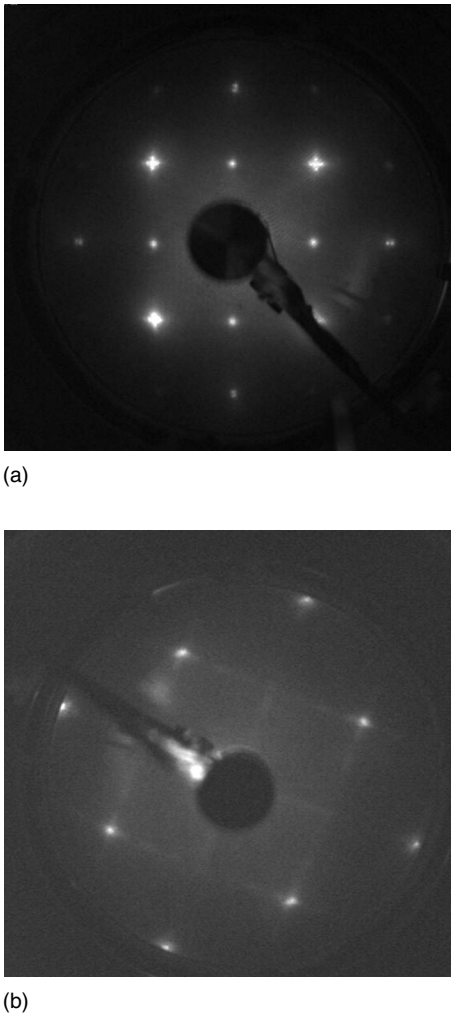

(a)

(b)

FIG. 1. LEED measurements of the N-covered Cu(100) surface. Top: the energy is set to $E = 129$ eV. Additionally, to the spots induced by the Cu substrate and by the $c(2 \times 2)$N overlayer, we observed spots belonging to the long distance periodicity of the islands. Bottom: the energy is set to $E = 39$ eV. At very high coverage, lines appear in the LEED image, reflecting the long trenches caused by surface stress.

peaks appear in the photoemission spectra. Figure 2 shows a few examples of photoemission spectra measured in different mirror planes of the crystal (ΓLUX and ΓXWK). The data represent spectral intensities, which we observed for different photon energies and for different polarization and electron emission angles. Deviations in the measured line shapes of spectral intensities that belong to the clean and to the N-covered surface indicate the presence of N-induced adsorbate states. In addition to peaks which originate from emission out of adsorbate bands, peaks due to umklapp processes have been observed. They can be identified by varying the photon energy. The spectra in Fig. 2 show various adsorbate peaks above and below the Cu d band complex that ranges in binding energy from $E_i = -2$ eV to $E_i = -5$ eV. Furthermore, an adsorbate band located in energy just within the Cu d band complex was found. By analyzing the different binding energies as a function of the electron emission angle and by taking into account the change of the work function, we were

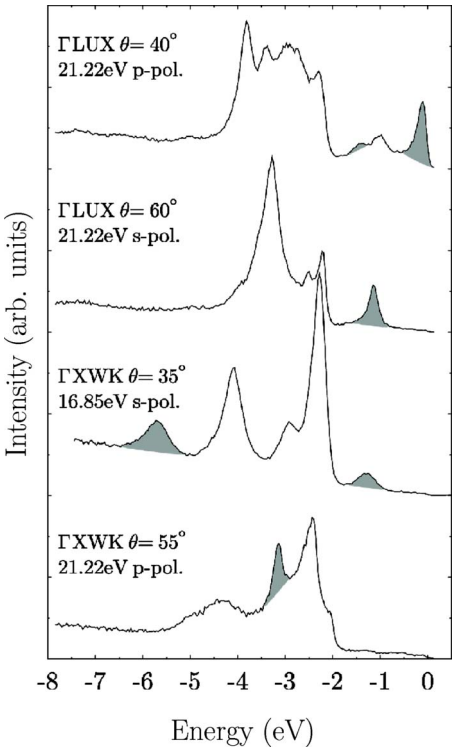

FIG. 2. (Color online) Photoemission spectra of the N-covered Cu(100) surface. The line shapes were measured in two different mirror planes for different electron detection angles θ, for different photon energies, and for different polarizations. The adsorbate-induced states are marked by gray color.

able to determine the dispersion relations of the different adsorbate states. Figure 3 shows the dispersion relations of the N-induced bands along $\bar{\Gamma}\bar{X}$ (ΓLUX in the volume) and $\bar{\Gamma}\bar{M}$ (ΓXWK). The $c(2\times2)$ overlayer structure induces a new symmetry-point $\bar{M}'$.

One of the occupied adsorbate-induced bands shows a strong dispersion from near $\bar{X}$ ($E_i \approx -7.5$ eV) to $\bar{\Gamma}$ ($E_i = -5.01$ eV) and finally to $\bar{M}'$ ($E_i = -5.72$ eV). The corresponding orbitals reveal an odd symmetry by excitation with *s*-polarized light. At $\bar{M}'$, the effective mass is $m^\star = +2.8m_0$ at $\bar{\Gamma}$ $m^\star = -1.2m_0$. The typical errors of the parameters in use are $\Delta E_i = \pm 0.02$ eV for the binding energy and $\Delta m^\star = \pm 0.1m_0$ for the effective mass.

Another state with odd symmetry is located in energy at $E_i = -4.76$ eV at $\bar{X}$. In addition to this band with bonding character, we were able to observe occupied antibonding bands located between the Cu *d* bands with lowest binding energy and the Fermi edge E_F ($E_i = 0$ eV). Along $\bar{\Gamma}\bar{M}'$, a band could be identified by excitation with *s* and *p*-polarized light as well. The symmetry character is found *xy*-like. The binding energy results in $E_i = -1.26$ eV at $\bar{M}'$ with an effective mass $m^\star = -1.5m_0$. The antibonding state with even symmetry disperses around $\bar{X}$ with $m^\star = -1.4m_0$. It seems to touch the Fermi energy with the tendency to cross E_F, but we were not able to decide this unambiguously from our measurements.

Furthermore, at lower binding energies, an odd state appears that has a binding energy $E_i = -1.42$ eV and an effective mass $m^\star = +1.5m_0$ at $\bar{X}$. A bonding state with even symmetry character could not be found from our measurements. In fact, it is very difficult to extract adsorbate-induced states with binding energies comparable to that of the Cu *d* band complex because of the strong overlap with the substrate states. Therefore, only one adsorbate-induced band with nearly vanishing dispersion around $\bar{M}'$ could be found with a binding energy $E_i = -3.13$ eV and even symmetry character. Finally, some other states with odd symmetry character could be identified for binding energies between $E_i = -3$ eV and $E_i = -5$ eV. These states show very weak dispersions as well.

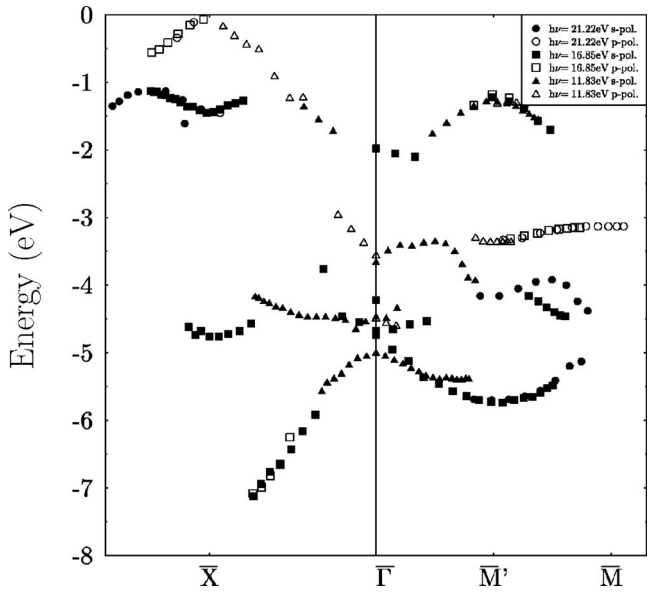

FIG. 3. Measured surface band structure of the adsorbate system N/Cu(100). The data points represent the corresponding binding energies E_i of the adsorbate peaks, which we obtained for different photon energies (○: $\hbar\omega = 21.22$ eV, □: 16.85 eV, and △: 11.83 eV) and different light polarizations (white symbols: *p* polarized; black symbols: *s* polarized).

The dispersion behavior of some of the adsorbate-induced states is very pronounced. This is untypical for surface emission from quasi-zero-dimensional islands. On the other hand, it was not possible for us to observe band splitting of the adsorbate bands into discrete eigenstates of the islands because the linewidth of the corresponding states is very large. For example, we measured typical linewidths of the adsorbate-induced peaks of about $\Gamma \approx 200$ meV. Such a linewidth corresponds to a very short lifetime and causes a short mean free path of the electrons. The mean free path λ itself can be calculated from the group velocity $v_g = \partial\omega/\partial k$ of the electrons multiplied by their lifetime $\tau = \hbar/\Gamma$ λ results in

$$\lambda = v_g \frac{\hbar}{\Gamma}. \tag{1}$$

The maximum group velocity can be estimated by the use of the maximum slope $\partial E/\partial k$ from the dispersion relations. For a typical linewidth $\Gamma = 200$ meV, the maximum mean free path is $\lambda = 13$ Å. Therefore, λ is much smaller than the island superstructure (≈ 50 Å). In other words, the influence of the

island boundaries is negligible for these strongly damped electronic states. In consequence, a splitting into discrete eigenstates is not expected for this system.

III. CALCULATIONAL DETAILS

A. Electronic structure

The electronic structure calculation has been performed in the framework of density functional theory (DFT), by using the full-potential augmented plane wave method with local orbitals, as implemented in the WIEN2K code.[16] A slab geometry was used, with a tetragonal unit cell of the dimensions $1\times1\times10$, in terms of the Cu-lattice constant, which is 6.84 a.u. The slab consists of 11 Cu layers with two atoms in each layer and one N layer on each side. A deviation from the undistorted fcc structure was introduced in the topmost Cu layer, corresponding to an outward relaxation of 4% of the interlayer distance. The N atom was placed 0.76 a.u. above the void in the outermost Cu layer or 4.296 a.u. above the Cu atom in the previous (unrelaxed) layer. This surface geometry has been taken from Ref. 15 and was not adjusted within the calculational procedure. The separation between the two N layers results in 32.245 a.u., presumably large enough to suppress the N-N "across the gap" interactions, as compared to N-N interactions between N atoms within a layer of the slab. The muffin-tin sphere sizes used in the calculation were fixed to 2.0 bohr for Cu and 1.45 bohr for the N atom. The generalized gradient approximation for exchange correlation has been used from Perdew–Burke–Ernzerhof.[17] The corresponding band structure that results from the calculational setup is presented in the following figure. Figure 4 shows a variety of Cu and N states within the surface Brillouin zone. It is clearly observable that the projected band gap existing at $\bar{\Gamma}$ for clean Cu(100) is suppressed in the case of a N-covered surface. This is caused by the umklapp process that takes place along $\overline{\Gamma M}$ through the influence of the $c(2\times2)$-overlayer structure. The electronic adsorbate states, which could be clearly identified in comparison with the experimental peak dispersions, have been marked by lines. For example, an adsorbate band with *xy*-like symmetry disperses from $\bar{X}$ at −7.5 eV binding energy to $\bar{\Gamma}$ at −5.0 eV and further onto the $\bar{M}'$ point at −6.0 eV. This band could be measured with *s*-polarized light, but it should be detectable also with *p*-polarized photons because of the degeneracy existing in both directions. Also, we observed along $\overline{\Gamma M}'$ an adsorbate state that disperses in accordance with the experiment from the top of the *d* band to the Fermi level. The symmetry is again *xy*-like. A third adsorbate band that has *z*-like symmetry could be identified just below the Fermi level at the $\bar{X}$ point. For energies related to the variety of Cu *d* bands, we were able to identify unambiguously adsorbate states that are not visible in the calculated band structure. Apart from this shortcoming of the calculations, a quantitative agreement between experiment and theory was found.

Simultaneously, the self-consistent electronic structure calculation has been performed by another DFT method, the so-called tight-binding linear muffin-tin orbital (TB-LMTO) method,[18–20] which employs space-filling atomic spheres with a spherically symmetric potential inside. These potentials have been used for the spectroscopical analysis. The geometrical setup in the TB-LMTO calculation is nearly identical to the one specified above. The only difference consists in the vacuum part of the slab that was build up by ten layers of empty spheres, respecting the fcc structure of Cu. The sphere radii have been fixed at 2.72 bohr for Cu, 1.41 bohr for N, and 1.63 up to 2.72 bohr for the different empty-sphere layers. The nonlocal correction to the exchange-correlation potential was treated by Langreth and Mehl.[21] The accuracy of the TB-LMTO method is normally inferior to a WIEN2K calculation when dealing with inhomogeneous or open structures. However, in our case, we were able to reproduce the band dispersions quantitatively. The clean Cu surface shows a projected band gap at $\bar{\Gamma}$ around $E_i>2$ eV.[22] The adsorption of N is responsible for the disappearance of the gap, since the overlayer $c(2\times2)$ structure allows umklapp processes with a new surface wave vector $\overline{\Gamma M}'$, as has been discussed before.[23,24]

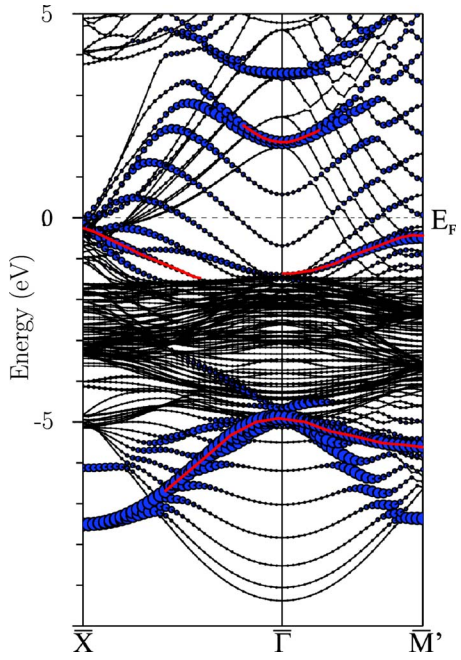

FIG. 4. (Color online) Calculated surface band structure of the adsorbate system Cu(200)$c(2\times2)$N. Surfacelike features have been indicated by filled dark (blue) circles. Electronic adsorbate states, which could be clearly identified in comparison with the experimental peak dispersions, have been marked by gray (red) lines.

B. Photoemission

In order to calculate relativistic photoemission intensities, we start in solving the Dirac equation,

$$\{c\hat{\boldsymbol{\alpha}}\mathbf{p}+\beta c^2+V(\mathbf{r})+\beta\hat{\boldsymbol{\sigma}}\mathbf{B}(\mathbf{r})-E\}\Psi(\mathbf{r})=0. \qquad (2)$$

In this expression, $V(\mathbf{r})$ denotes the effective potential and $\mathbf{B}(\mathbf{r})$ is the effective magnetic field. β is a 4×4 matrix that fulfills $\beta^2=1$ and $\hat{\alpha}$ is a 4×4 Dirac matrix, which is defined by the 2×2 Pauli matrices σ_k $[\alpha_k=\sigma_x\otimes\sigma_k, (k=x,y,z)]$. The

Dirac equation itself can be obtained from the relativistic generalization of density functional theory introduced by Rajagopal and co-workers.[25,26] It can be solved using the phase-functional ansatz of Calogero *et al.*[27] generalized to the relativistic case.[28–31] From this solution, it is easy to define the atomic scattering matrix Γ for a single ion-core potential together with the wave functions for the initial and for the final states. The atomic scattering matrix Γ together with the crystal geometry determines the scattering matrix M for a single layer. By means of layer-doubling techniques, the so-called bulk-reflection matrix can be calculated, which gives the scattering properties of a semi-infinite stack of layers. Finally, applying the spin polarized LEED theory,[32–40] we are able to derive the final state and the initial state for the semi-infinite crystal. The relativistic form of the four different contributions to the photocurrent, originally introduced by Pendry,[41] has been described in detail in Ref. 42 and 43. Therefore, we restrict ourselves to giving some remarks on the computational details of the photoemission calculations.[43] Lifetime effects in the final and initial states have been included in our analysis in a phenomenological way by using a parameterized complex inner potential $V_o(E) = V_{or}(E) + iV_{oi}(E)$. Herein, the real part serves as a reference energy inside the crystal with respect to the vacuum level. For the final state, a constant imaginary part $V_{oi}(E_2) = 1.8$ eV has been chosen. For the initial state, we decided for the following energy dependence of V_{oi},

$$V_{oi}(E_1) = \arctan[0.05 + 0.001(E_1 - E_F)^2 + 0.001(E_1 - E_F)^4], \tag{3}$$

with E_1 in eV. For the photoemission analysis, we used the layer-dependent potential that was calculated in the framework of the TB-LMTO method.[18,44] The details have been discussed in the previous section. A realistic description of the surface potential is given through a spin-dependent Malmström–Rundgren barrier,[45] which connects the asymptotic regime $z < z_A$ to the bulk muffin-tin zero V_{or} by a third order polynomial in z. The corresponding parameters have been chosen equal to those which were established for pure Cu(100). Additionally, the calculated intensity distributions have been multiplied with the Fermi function and convoluted with a Gaussian of full width at half maximum =0.05 eV to account for the finite resolution of the experiment. Furthermore, we used a lattice constant of 6.95 a.u. for the system Cu(100)(2×2)N instead of the usual lattice constant for bulk Cu, which is 6.84 a.u. This is due to the experimental finding that the lattice constant is enhanced by the adsorbtion of N on the surface. The value ϕ=4.59 for the work function of the clean Cu surface has been taken from Gartland *et al.*[46] For the N-covered surface, we used the measured value of 5.07 eV.

Caused by the coverage with N, a volume state, the Cu *sp* band, is shifted to lower binding energies. For low photon energies ($\hbar\omega$=11.83 eV), the *sp* band can be observed in normal emission θ=0° (Fig. 5). In this case, the change of the work function due to the adsorption of N cannot affect the peak position. Therefore, the energetic shift is caused by the N-induced change of the lattice constant within the Cu surface. This happens because the umklapp processes in the surface contribute to the transition ($\vec{k}_f = \vec{k}_i + \vec{G}$). Since the band dispersion of the peak is well known,[24] the change in the lattice constant is extractable from the measured change in the binding energy that is ΔE=150 meV. In fact, we found that the lattice constant is enhanced to 6.95 a.u. (Fig. 5). The other bulklike states of Cu were not so strongly affected because their dispersional behavior is much less pronounced.

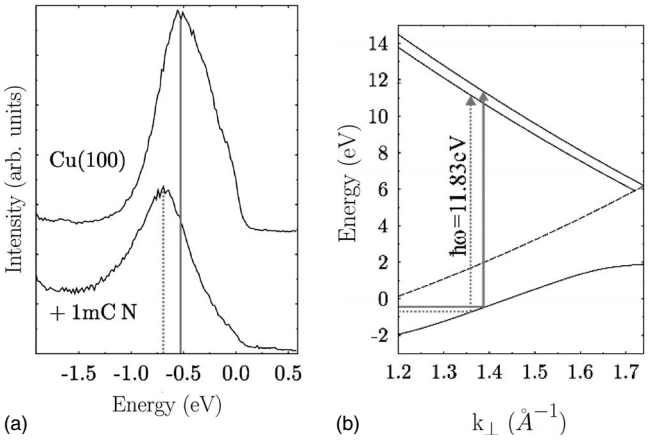

FIG. 5. The *sp*-band peak measured in normal emission with $\hbar\omega$=11.83 eV. Even due to a low coverage with N, the photoemission peak is shifted to lower binding energies (left panel). The reason is the change of the wave vector due to the N coverage. Stress induces a change of the lattice constant. As umklapp processes in the surface contribute to the photoemission process, the change of the reciprocal lattice constant causes a shift of the binding energy (right panel).

We accounted for the proposed outward relaxation of the first layer by using 2.5% of the lattice constant. Also, rumpling of Cu and N atoms within this layer has been considered in the calculations. The effect of atomic rumpling on the spectral line shapes and, in consequence, the influence of rumpling on the geometric surface structure will be discussed in more detail in the next section.

IV. DISCUSSION

We compared two different types of surface reconstructions. The first one consists of a surface layer with strong outward relaxation and rumpling of the N atoms only. In the second case, we additionally considered rumpling in the Cu atoms of the surface layer. In Fig. 6, an angle-dependent series of measured and calculated photoelectron spectra is shown for emission along the ΓLUX and ΓXWK directions of the surface Brillouin zone as a function of energy and polarization of the incoming photons. A first inspection on the different line shapes of experimental and theoretical data reveals a more or less quantitative agreement in the energetics for all spectra. This is also observable for the spectra shown in Fig. 7, in which combined N and Cu rumpling has been taken into account. In consequence, this tells us that surface rumpling is not able to influence the energetic positions of bulklike structures too much. This theoretical finding is in accordance with test calculations that had been per-

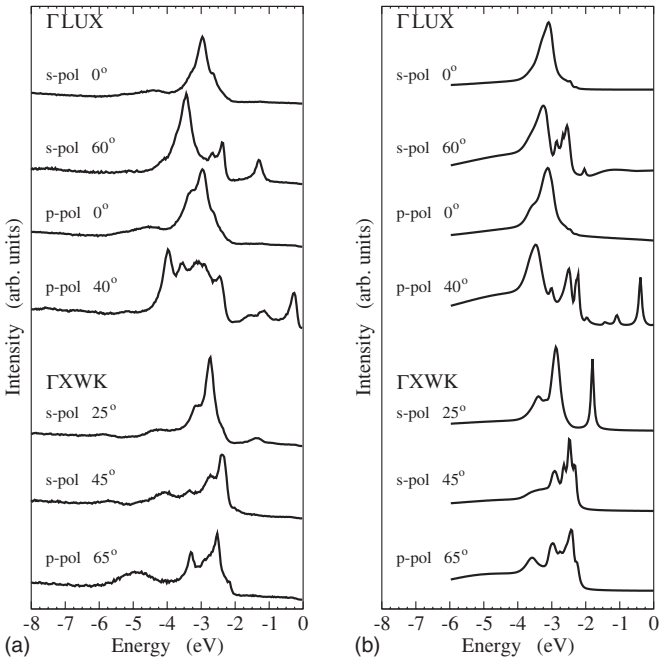

FIG. 6. Measured (left) and calculated (right) photoemission spectra obtained for an excitation energy of $\hbar\omega=21.22$ eV from the N-covered Cu(100) surface. In the theory, rumpling of N atoms has been considered only. According to the experiment, the spectra were calculated for two different mirror planes and for different electron detection angles θ as a function of photon energy and polarization.

formed on a pure Cu(100) surface before. On the other hand, surface or adsorbate states are significantly influenced in their energetic behavior as well as in their intensity distributions when changing the surface geometry. For example, in Fig. 6, the N-induced state that occurs at about 1.2 eV binding energy in the experimental data obtained for *s*-polarized light at 60° off-normal emission is not present in the corresponding theoretical spectrum. A more close inspection, of course, reveals a variety of deviations in the different line shapes of the experimental and theoretical spectra shown in Fig. 6. Introducing Cu rumpling in the first layer, the agreement concerning the different intensity distributions is improved on a quantitative level. At first, the N-induced adsorbate state appears in the calculated spectrum (*s* polarized, 60°, Γ*LUX*) at the measured binding energy with the correct relative intensity. Only the lifetime is underestimated by the calculation. Furthermore, the intensity and energetic position of the adsorbate state measured at 1.3 eV binding energy with *s*-polarized light at $\theta=25°$ off-normal emission along Γ*XWK* is in much better agreement with the calculation when rumpling of Cu atoms is taken into account. These observations clearly favor the geometric structure model inhibiting the lower surface symmetry that was proposed first by Hoeft and co-workers.[13,15] Nevertheless, there are deviations observable in the line shapes that cannot be accounted for even by applying a combined rumpling of N and Cu atoms. Further improvements may be expected through surface-sensitive electronic structure methods such as the tight-binding Korringa–Kohn–Rostoker approach. Also, the application of the full-potential photoemission theory seems to be necessary. This work will be done in a future investigation.

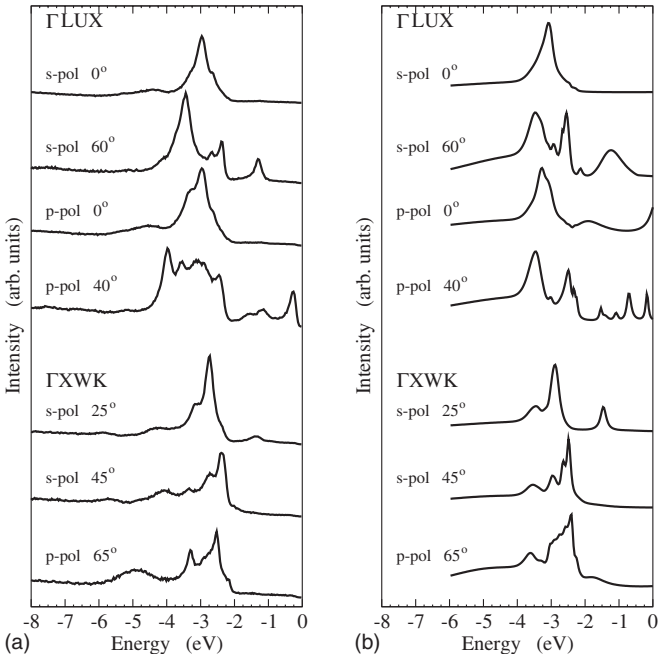

FIG. 7. Comparison of measured (left) and calculated (right) photoemission spectra. The theoretical spectra have been calculated with rumpling of N and Cu atoms.

V. SUMMARY

We have presented a detailed investigation on the electronic and geometric structure of the adsorbate system N/Cu(100). For all coverages, a sharp $c(2\times2)$ LEED pattern was found. For low N coverages, square N islands appear indicated by additional features in the LEED pictures. The photoemission distributions measured with linear polarized light reveal a strong dispersion of the N adsorbate states, which is due to the dimensionality of the corresponding islands.

Furthermore, we compared our experimental results with first principles electronic structure and photoemission calculations to guarantee for a quantitative analysis. The calculated surface band structure nicely shows the dispersion of N-induced states, which were found to be in a very good agreement with the measured energetics. The comparison of experimental and theoretical photoemission line shapes favors as a structural model for N/Cu(100) a rumpled surface with a twofold symmetry.

ACKNOWLEDGMENTS

Financial support from the Deutsche Forschungsgemeinschaft is gratefully acknowledged. This work was supported in part by the BMBF within the Verbundprojekt "Elektronische Struktur und Photoemission von Hochkorrelierten Intermetallischen Seltenen Erdverbindungen" (Contract No. 05605MPA0).

[1] F. M. Leibsle, C. F. J. Flipse, and A. W. Robinson, Phys. Rev. B **47**, 15865 (1993).
[2] J. M. Gallego, S. Y. Grachev, M. C. G. Passeggi, Jr., F. Sacharowitz, D. Ecija, R. Miranda, and D. O. Boerma, Phys. Rev. B **69**, 121404(R) (2004).
[3] H. Miyaoka, N. Kawamura, T. Iimori, and F. Komori, Thin Solid Films **464-465**, 260 (2004).
[4] L. Triguero and L. G. M. Pettersson, Surf. Sci. **398**, 70 (1998).
[5] T. Wiell, J. E. Klepeis, P. Bennich, O. Björneholm, N. Wassdahl, and A. Nilsson, Phys. Rev. B **58**, 1655 (1998).
[6] F. M. Leibsle, S. S. Deshi, S. D. Barrett, and A. W. Robinson, Surf. Sci. **317**, 309 (1994).
[7] F. Komori, S. Ohno, and K. Nakatsuji, Prog. Surf. Sci. **77**, 1 (2004).
[8] S. Ohno, K. Yaguu, K. Nakatsuji, and F. Komori, Surf. Sci. **547**, L871 (2003).
[9] M. Sotto and B. Croset, Surf. Sci. **461**, 78 (2000).
[10] H. C. Zeng, R. N. S. Sodhi, and K. A. R. Mitchell, Surf. Sci. **188**, 599 (1987).
[11] T. Lederer, D. Arvanitis, M. Tischer, G. Comelli, L. Tröger, and K. Baberschke, Phys. Rev. B **48**, 11277 (1993).
[12] Q. Dai and A. J. Gellman, Surf. Sci. **248**, 86 (1991).
[13] J. T. Hoeft, M. Polcik, M. Kittel, R. Terborg, R. L. Toomes, J.-H. Kang, and D. P. Woodruff, Surf. Sci. **492**, 1 (2001).
[14] T. E. Wofford, S. M. York, and F. M. Leibsle, Surf. Sci. **522**, 47 (2003).
[15] S. M. Driver, J. T. Hoeft, M. Polcik, M. Kittel, R. Terborg, R. L. Toomes, J.-H. Kang, and D. P. Woodruff, J. Phys.: Condens. Matter **13**, L601 (2001).
[16] P. Blaha, K. Schwarz, P. Sorantin, and S. B. Trickey, Comput. Phys. Commun. **59**, 339 (1990).
[17] J. P. Perdew, K. Burke, and M. Ernzerhof, Phys. Rev. Lett. **77**, 3865 (1996).
[18] O. K. Andersen and O. Jepsen, Phys. Rev. Lett. **53**, 2571 (1984).
[19] O. K. Andersen, O. Jepsen, and M. Sob, in *Linearized Band-structure Methods*, edited by M. Yussouff, Lecture Notes in Physics (Springer-Verlag, Berlin, 1987).
[20] O. K. Andersen, T. Saha-Dasgupta, R. W. Tank, C. Arcangeli, O. Jepsen, and G. Krier, *Developing the MTO Formalism in Electronic Structure and Physical Properties of Solids: The Uses of the LMTO Method*, edited by Hugues Dreyss, Lecture Notes in Physics (Springer-Verlag, Berlin, 2000).
[21] D. C. Langreth and M. J. Mehl, Phys. Rev. B **28**, 1809 (1983).
[22] S. L. Hulbert, P. D. Johnson, M. Weinert, and R. F. Garrett, Phys. Rev. B **33**, 760 (1986).
[23] R. W. G. Wyckoff, *Crystal Structures*, 2nd ed. (Interscience, New York, 1963).
[24] H. Eckhardt, L. Fritsche, and J. Noffke, J. Phys. F: Met. Phys. **14**, 97 (1984).
[25] A. K. Rajagopal and J. Callaway, Phys. Rev. B **7**, 1912 (1973).
[26] M. V. Ramana and A. K. Rajagopal, Adv. Chem. Phys. **54**, 231 (1983).
[27] F. Calogero, *Variable Phase Approach to Potential Scattering* (Academic, New York, 1967).
[28] H. Ebert and B. L. Gyorffy, J. Phys. F: Met. Phys. **18**, 451 (1988).
[29] A. Gonis, *Green Functions for Ordered and Disordered Systems: Studies in Mathematical Physics* (North-Holland, Amsterdam, 1992), Vol. 4.
[30] X. Wang, X. G. Zhang, W. H. Butler, G. M. Stocks, and B. N. Harmon, Phys. Rev. B **46**, 9352 (1992).
[31] S. C. Lovatt, B. L. Gyorffy, and G. Y. Guo, J. Phys.: Condens. Matter **5**, 8005 (1993).
[32] W. Kohn and N. Rostoker, Phys. Rev. **94**, 1111 (1954).
[33] A. R. Williams and J. van W. Morgan, J. Phys. C **7**, 37 (1974).
[34] R. Feder, J. Phys. C **14**, 2049 (1981).
[35] R. G. Brown and M. Ciftan, Phys. Rev. B **27**, 4564 (1983).
[36] A. Gonis, X. G. Zhang, and D. M. Nicholson, Phys. Rev. B **40**, 947 (1989).
[37] X. G. Zhang, A. Gonis, and J. M. MacLaren, Phys. Rev. B **40**, 3694 (1989).
[38] W. H. Butler and R. K. Nesbet, Phys. Rev. B **42**, 1518 (1990).
[39] R. K. Nesbet, Phys. Rev. B **41**, 4948 (1990).
[40] W. H. Butler, A. Gonis, and X. G. Zhang, Phys. Rev. B **45**, 11527 (1992).
[41] J. B. Pendry, Surf. Sci. **57**, 679 (1976); J. F. L. Hopkinson, J. B. Pendry, and D. J. Titterington, Comput. Phys. Commun. **5**, 599 (1980).
[42] J. Braun, Rep. Prog. Phys. **59**, 1267 (1996).
[43] M. Grass, J. Braun, G. Borstel, R. Schneider, H. Dürr, Th. Fauster, and V. Dose, J. Phys.: Condens. Matter **5**, 599 (1993).
[44] O. K. Andersen, Phys. Rev. B **12**, 3060 (1975).
[45] G. Malmström and J. Rundgren, Comput. Phys. Commun. **19**, 263 (1980).
[46] P. O. Gartland, S. Berge, and B. J. Slagsvold, Phys. Rev. Lett. **28**, 738 (1972).